Research article

X-RAY Spectrometry

Received: 8 November 2011 Revised: 15 September 2012 Accepted: 16 October 2012 Published online in Wiley Online Library: 20 November 2012

(wileyonlinelibrary.com) DOI 10.1002/xrs.2433

A new application of X-ray scattering using principal component analysis – classification and identification of liquid precursor chemicals

Yu Zhong,[a,b†] Fang Zhang,[a†] Wei Li,[a] Minqiang Li,[a] Bai Sun,[a] Yu Zhang,[a] Daoyang Yu[a]* and Jinhuai Liu[a]*

X-ray scattering (XRS) combined with principal component analysis has been utilized for classifying and identifying liquid precursor chemicals for the first time. The XRS spectra of some liquid precursor chemicals and normal materials were obtained by using an XRS system, and the profiles of scattering media distinctly reveal that the XRS spectra are unique corresponding to the specific liquid material. Furthermore, the obtained spectra were processed through principal component analysis by using the selected energy region in the spectra. The score plots of each substance were clustered together and almost coincident for the same liquid, implying good repeatability and reliability. As far as the different liquid materials are concerned, they could be classified into distinct groups according to their positions in the score plot. The score plots showed a clear classification and recognition of liquid precursor chemicals. This study demonstrates a possibility for analyzing different liquid materials, and it presents a new application for X-ray spectroscopy.

Introduction

Since the 1980s, transnational smuggling and trafficking of precursor chemicals have increased rapidly in tandem with the prevalence of the global drug problem and the extended production of chemo-synthesized drugs.[1] The precursor chemicals can be used in the illicit manufacture of narcotic drugs and psychotrophic substances. A variety of liquid precursor chemicals are required for the illicit manufacture of amphetamines and other synthetic drugs and for the illicit processing of cocaine and heroin. For example, safrole and isosafroles are employed to manufacture 3,4-methylenedioxy-methamphetamine as starting materials, acetone is utilized to refine cocaine, and acetic anhydride has an application as heroin processing.

Recently, many approaches have been proposed to address the challenge of liquid precursor chemical identification for the monitoring and controlling of the precursor chemical security screening. Unfortunately, some of them have different disadvantages and deficiencies. For example, the techniques of gas chromatography coupled with mass spectrometry and ion mobility spectrometry are relatively expensive and required sophisticated instrumentation, and the recognition method of chemical color tests requires a variety of chemical reagents and multiple-step tests to obtain the results, in which quick identification is difficult to achieve.[2–5] Furthermore, those approaches require direct contact with the liquid samples generally hidden in containers that cannot be opened routinely for inspection.

X-ray scattering (XRS) is well known for its ability to identify substance in a fast, simple, low-cost, nondestructive, and noninvasive way, especially using its radiation that is sufficiently penetrating to a parcel or containers containing other attenuating media and producing profiles that are substance specific.[6–8] XRS has been widely employed in the structural characterization of amorphous samples and liquids[9,10] and potentially enables the analysis of the disordered systems.[11,12] Its particular geometric properties allow the placement of liquid samples stored in sealed cells and much shorter acquisition times than those typical of any other in-house apparatus. When dealing with liquid samples, XRS effects are highly matrix dependent. There are three XRS effects after the interaction of liquid samples with X-ray incident beam, namely Rayleigh (or coherent) scattering, Compton (or incoherent) scattering, and X-ray Raman scattering.[13] The scattering effect characteristics of the scattering media are superimposed upon the continuous spectrum of primary X-ray spectrum to produce a unique scattering profile.[14]

According to the Bragg's law, the scattering profile is expressed as a function of momentum transfer, q, which depends on scattering angle θ and photon energy E as follows[15,16]:

$$q = \frac{1}{\lambda}\sin\left(\frac{\theta}{2}\right) = \frac{E}{hc}\sin\left(\frac{\theta}{2}\right) \quad (1)$$

where λ, h, and c are the wavelength of the incident radiation, the Planck's constant, and the speed of light, respectively. When E is expressed in kiloelectron volt, the unit of momentum transfer q is reciprocal nanometer. It is apparent that the material structure can be interrogated either by holding λ fixed or by

* *Correspondence to: Daoyang Yu, Key Laboratory of Biomimetic Sensing and Advanced Robot Technology, Institute of Intelligent Machines, Chinese Academy of Sciences, Hefei, Anhui 230031, China. E-mail: ydy@iim.ac.cn*
Jinhuai Liu, Key Laboratory of Biomimetic Sensing and Advanced Robot Technology, Institute of Intelligent Machines, Chinese Academy of Sciences, Hefei, Anhui 230031, China. E-mail: jhliu@iim.ac.cn

† *These two authors contributed equally to this work.*

a *Key Laboratory of Biomimetic Sensing and Advanced Robot Technology, Institute of Intelligent Machines, Chinese Academy of Sciences, Hefei, Anhui, 230031, China*

b *Anhui Provincial Laboratory of Biomimetic Sensor and Detecting Technology, West Anhui University, Anhui, Lu'an, 237012, China*

measuring the scattering as a function of θ. It is generally known as angular dispersive diffraction technique, and the method is used in most standard diffraction measurements or in an energy-dispersive mode whereby measurements are made at a fixed scattering angle θ while using a broad energy band polychromatic X-ray beam, which is defined as polychromatic or white. The energy spectrum of the scattered radiation is acquired by an energy-sensitive detector, no movements being required. This technique requires an energy-resolving detector to measure simultaneously a range of scattered photon energies.

The XRS spectra, because of its characters of high-dimensional data, are difficult to cope with. The features of scattering data can be studied when chemometrics is employed. One of the most useful and well-established chemometric tools is principal component analysis (PCA). PCA is the principal base of modern methods of treating multivariate data.[17] PCA summarizes the information of the initial data set into a new set, which is smaller than the former. This new data set contains only the relevant statistical information, built onto a new system of axes that represent the samples, making it possible to visualize the multivariate characteristics of the data in a few dimensions. In other words, PCA can be seen as a projection of the data onto a lower dimensional subspace, maximizing variance.

Principal component analysis is known as an effective method of feature extraction. Let $X \sim F$ be a p-dimensional random vector with covariance matrix V, and let F^a be the distribution function of $a'X$, where a is a p vector. Denote the eigenvalues of V by $r_1, \ldots, r_p$. The first principal component is the projection of X onto a certain direction:

$$\sigma(F^{a_1}) = \max_{\|a\|=1} \sigma(F^a) = \max_{\|a\|=1} (a'Va)^{1/2}$$

As we know, $\sigma^2(F^{a_1}) = a_1{}'Va_1$ is the largest eigenvalue r_1 and that a_1 is the associated eigenvector. Similarly, the kth principal component $a_k{}'X$ is defined by

$$\sigma(F^{a_k}) = \max_{\|a\|=1, a\perp a_1, \ldots, a\perp a_{k-1}} \sigma(F^a)$$

Thus, one concludes that $\sigma^k(F^{a_k}) = r_k$ and that a_k is the eigenvector associated with r_k. Here, PCA is searching for low-dimensional projection index. On the other hand, if the principal components of V are known, V can be constructed by $V = \sum r_i a_i a_i{}'$.

Principal component analysis promotes dimension reduction of the original data, modeling of data, selection of main variables, and classification of samples.[18,19] PCA creates new coordinate axes (named principal components) from the original data. This characteristic is especially important when spectra are studied, as it helps to visualize and to extract information from this type of data by applying PCA.[20–22]

The present study describes the use of XRS combined with PCA to classify and identify liquid precursor chemicals. First of all, the XRS spectra of liquid precursor chemicals were measured and obtained using a noncommercial energy-scanning apparatus, which is the advantages and attractive aspects of nondestructivity and easy-to-perform technique. Secondly, XRS spectra of liquid precursor chemicals were analyzed. Thirdly, after being truncated, denoised, and autoscaled, the spectra were analyzed by PCA, which is useful in feature extraction and dimension reduction in high-dimensional and intercorrelated data. Finally, a classification and identification method based on XRS and PCA was set up.

Experimental

Instrumentation

The experiments were performed by using the noncommercial energy-scanning diffractometer built in the Institute of Intelligent Machines, Chinese Academy of Sciences.[12,23] The XRS equipment consisted of (1) a Seifert X-ray generator, (2) a water-cooled tungsten X-ray source with 3.0 kW maximum power and a nominal focal spot of 1×10 mm, (3) a silicon drift detector (XR-100SDD), which is connected to a multichannel analyzer (AMPTEK PX4, 1024) channels by an electronic chain for scattering spectra collection, which has an energy detection of 0.14 keV at 5.9 keV (^{55}Fe), (4) a collimator system that focuses the X-ray beam in front of and behind the sample, (5) a step motor for moving the arms to support the detector, whose minimum step movement leads to a minimum angle incrementum and reproduction of 0.01°, and (6) an adjustable sample holder that was positioned in the optical center of the diffractometer.

A schematic diagram of the experimental system is shown in Fig. 1. The distance between the X-ray source and the sample is 180 mm, and the distance between the sample and the detector is 120 mm. Two vertical slits 15 mm in height and of variable slit width collimate a parallel beam onto the sample, and a 0.02 mm in width and 15 mm in height receiving slit, which improve the angular resolution, collimates the scattered beam. The measurement was taken at a fixed scattering angle θ by using a white incident polychromatic beam.

Reagents

Twelve kinds of liquid samples including precursor chemicals and normal materials were used in this study: deionized water,

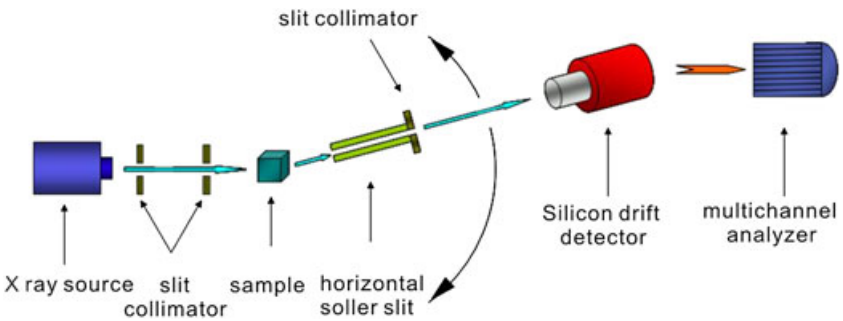

Figure 1. Sketch of the X-ray scattering spectrometer.

3,4-methylenedioxyphenyl-2-propanone, benzene, methylbenzene, *o*-xylene, acetone, 2-butanone, acetic acid, acetic anhydride, oil of vitriol, isosafrole, and ethyl ether. Except deionized water, all reagents were analytically pure grade. Each sample was repeatedly measured for four times at room temperature.

Results and discussion

Optimization of scattering conditions

In the experiment, the tungsten tube works at 55 kV and 20 mA, thus producing a white spectrum in the low energy range (the bremsstrahlung component of the X-ray source was used). The samples of the test liquid were sealed in a lucite holder with a capacity of 2.0 ml of sample and wall thickness of 70 um, which can avoid evaporation and contamination by moisture in the air. The liquid samples were exposed to X-rays for 3 min. The measuring time was set as 3 min, and 200–12,000 counts for each sample can be obtained. The large amount of counts significantly improved signal-to-noise ratio.

When the scattering angle between X-ray incident beam and exit beam is different, there are some differences in the intensity and shape distribution of X-ray spectrum.[24] After the interaction of liquid samples with X-ray incident beam, the local features of scattering spectra, which superimposed upon the continuous spectrum of primary X-ray spectrum, changed at different scattering angles. To search for an appropriate scattering angle, the change law of local features on the scattering curves was investigated at the different scattering angle. The selection of scattering angle is of critical importance and will affect the resolution, energy, and intensity of the scattering profiles. Scattering angles in the low range considered as the amorphous materials to be investigated and identified are known from literature.[15,25–27] The optimal scatter angle was selected by measuring the spectra of four liquid samples by using the 5°, 7°, and 9° scattering cells. The XRS spectra of benzene, acetone, methylbenzene, and 3,4-methylenedioxyphenyl-2-propanone are shown in Fig. 2. The *x*-coordinate represents 1024 channels of multichannel analyzer, equivalent in energy spectrum of 0–55 keV; the *y*-coordinate represents the number of photons in each channel, equivalent in counts of photon.

As seen from Fig. 2, four kinds of liquid materials illustrate different scattering curves at 5°, 7°, and 9°. As the formula (1) states that $\sin(\theta/2) \propto E^{-1}$, increasing the scatter angle θ compresses the scattering profile and shifts peak positions to lower energies. Also, increasing the scatter angle decreases the absolute width of each spectrum, which indicates that larger scatter angles are preferable. However, as the aim of the XRS system is to detect liquid materials in containers, which may be contained by other attenuating materials, the peaks should not be shifted much below 20 keV as lower energy X-rays are attenuated more.[28] At the same time, increasing the scatter angle, the scattering profiles may be severely disturbed by the transmitted primary beam. Thus, scatter angles of 9° and above are not considered. On the other hand, it can be seen that at angles of 5° and below, the information in all spectra, with the exception of the broad scattering pattern, the intensity and efficiency of photon counts are decreased seriously. Therefore, a scatter angle of 7° was chosen because it gave the best peak shape with appropriate count rates and energy. All the following work was carried out at this angle.

The X-ray intensity of an empty lucite holder and deionized water was measured to interrogate the influence of container scattering. As shown in Fig. 3, the XRS spectra of empty lucite holder and deionized water sample sealed in the lucite holder were measured at the scattering angle of 7°. As indicated in Fig. 3(a), there are only a few counts of photons in all energy coordinates except the fluorescence profiles of tungsten tube below

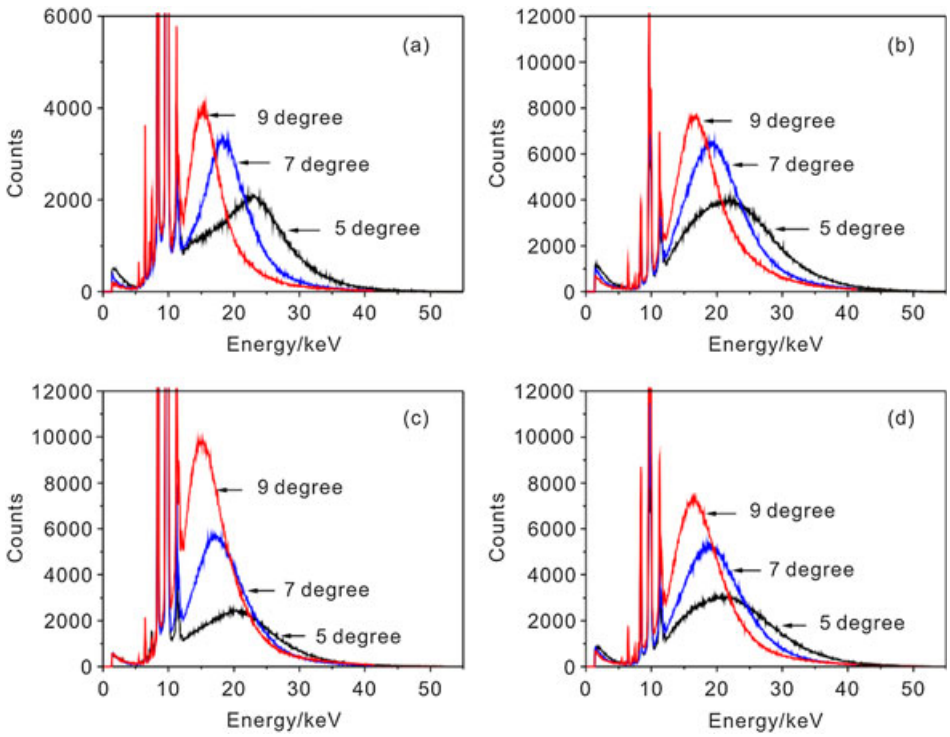

Figure 2. Scattering spectra of liquids at scatter angles of 5°, 7°, and 9°: (a) benzene, (b) acetone, (c) methylbenzene, and (d) 3,4-methylenedioxyphenyl-2-propanone.

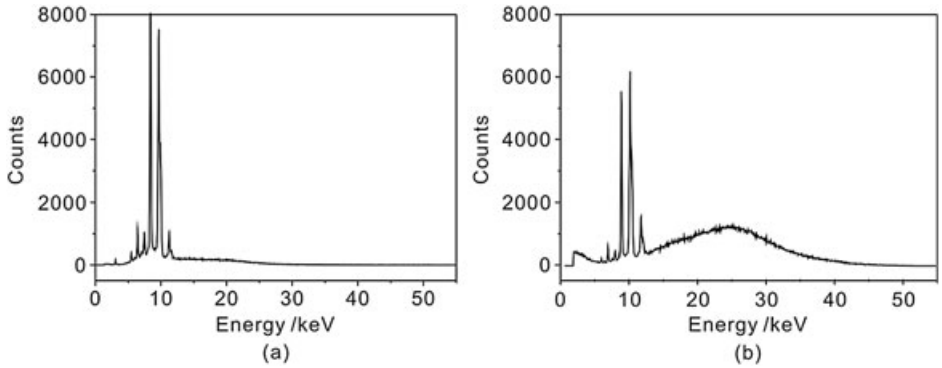

Figure 3. Scattering spectra of (a) the empty holder and (b) deionized water at scatter angles of 7°.

the 12 keV. This indicated that only a few photons were scattered and received by the detector when the X-rays penetrated the holder. The spectrum obtained for deionized water sample sealed in the lucite holder under the same condition is shown in Fig. 3(b). It can be seen that there are about 1200 photons at the maximal peak of scattering curves for deionized water. Therefore, the lucite holder almost did not affect the scattering spectra of the samples in the lucite holder.

Spectral analysis of ketone compounds and acids

In the present investigation, several kinds of precursor chemicals and normal materials in liquid state were measured on the same condition. The features of the XRS spectra are unique to the particular material, and there are significant differences among spectra of different kinds of liquid substances. The XRS spectra of acetone, 2-butanone, and 3,4-methylenedioxyphenyl-2-propanone are shown in Fig. 4(a). Their main peak is centered on 0.8 nm^{-1}, and each of them clearly produces its own distinct pattern of spectrum under the same experimental conditions. The shapes of experimental scattering curves for ketone compounds are similar, but their maximal peak positions are slightly different; furthermore, the difference of their scattering intensity is evident. The peak amplitudes and width of profiles gradually decrease with increasing the atomic numbers of carbon. Figure 4(b) shows scattering curves obtained with acetic acid, acetic anhydride, and oil of vitriol. As indicated in Fig. 4(b), the curves of acids are similar with those of ketone compounds, indicating that each acid clearly produces its own distinct pattern of the XRS spectra. The scattering position of acetic acid is in low energy range, accompanied with small q and low photon counts. The differences of the spectra between acetic acid and acetic anhydride are still obvious; although their maximal peak positions are extremely alike with each other, the difference of their scattering intensities is very evident. The shape, peak position, and scattering intensity of the scattering curves for oil of vitriol are greatly different among the experimental acids. One feature of Fig. 4(b) deserves special mention. The fluorescence profiles of tungsten tube are absorbed much more intensively by oil of vitriol than by acetic acid and acetic anhydride. In particular, the oil of vitriol clearly indicates the almost full absorption of tungsten anode characteristic line. The reason would be the presence of sulfur element of molecular structure. Compared with the atom of carbon, hydrogen, and oxygen in acetic acid and acetic anhydride, sulfur is a heavy element. The liquid materials containing heavy atoms would show more absorption effect of the fluorescence profiles of tungsten tube.

The spectral analysis of ketone compounds and acids indicates that liquids do not exhibit the sharp Bragg peaks presented by crystalline specimen. Instead, they show more or less structureless X-ray diffraction patterns consisting of weaker, broader features still to be observed.[6] Under the identical test conditions, the different liquids present a unique scattering spectrum containing the position, shape, width, and intensity of a series of peaks that are governed by the liquid properties.

Data analysis based on principal component analysis

On the basis of the aforementioned analysis, there are significant differences among the XRS spectra of most liquid precursor

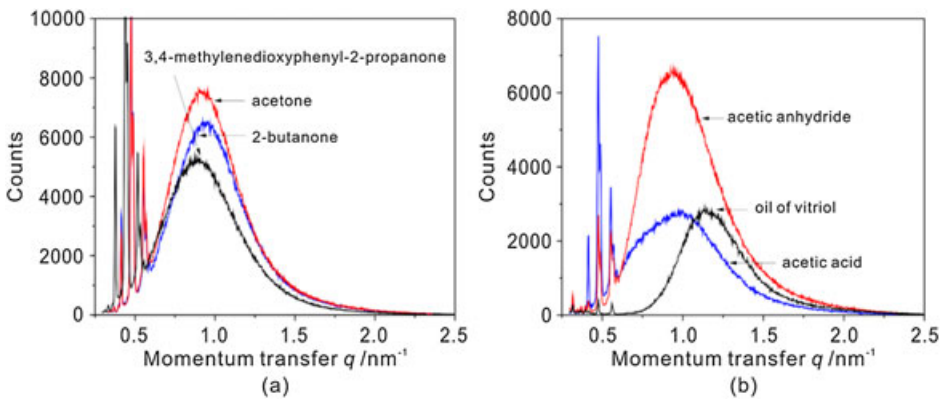

Figure 4. X-ray scattering spectra of (a) 3,4-methylenedioxyphenyl-2-propanone, acetone, and 2-butanone, and (b) acetic acid, acetic anhydride, and oil of vitriol.

chemicals. The amplitudes of the spectra are different, and peaks arise at different positions and energies. Most liquid precursor chemicals can be identified easily and intuitively from their XRS spectra. However, there still are some liquid precursor chemicals whose spectra are very similar, for example, spectra of acetone, 2-butanone, and 3,4-methylenedioxyphenyl-2-propanone in Fig. 4(a) and acetic acid and oil of vitriol in Fig. 4(b). Meanwhile, the intensity of XRS spectra is affected by many experimental conditions, so it is not a qualitative indication to distinguish liquid materials. In this section, a chemometric tool based on PCA is applied to identify and classify some liquid precursor chemicals with very similar XRS spectra.

Considering that the aim of this work is to identify and classify different kinds of liquid samples on the basis of distinct XRS profiles and PCA, the first step of data preprocessing was to select the appropriate region of XRS for this application. Figure 5(a) shows the original XRS spectral region for six kinds of different liquids (ethyl ether, isosafrole, acetic anhydride, 3,4-methylenedioxyphenyl-2-propanone, methylbenzene, and oil of vitriol). In Fig. 5(b), the region between 11.93 and 42.13 keV (from 201 to 712 channels) was chosen to focus on the key features of tested materials and reduce the computational complexity. After that, the data were subjected to PCA. The spectral data were processed via MATLAB® software.

Oil of vitriol and acetic anhydride are the liquids of precursor chemicals. All of tested acids are able to be separated into distinct groups, as shown in Fig. 6. A score plot of PC1 against PC2 by PCA is shown in Fig. 6, with 80.0% of the variance explained in PC1 and 19.0% in PC2. Another set of liquid precursor chemicals, three kinds of ketone compounds, was processed. The spectra obtained are presented in Fig. 4(a), where the similarities among the profiles are clear. Treating the data by PCA, it is possible to separate the ketones into groups, according to their chemical properties, as shown in Fig. 7. The high intensity of XRS furnished a better classification in the PC1 × PC2 score plot. It is shown that PCA can differentiate the ketone materials with 87.6% of the explained variance in PC1 and 6.7% in PC2. Benzene homologues are aromatic hydrocarbons, and methylbenzene is a precursor chemical among them. After PCA processing, it is possible to observe that a satisfactory separation is reached for three types of different benzene homologue samples in Fig. 8. A total of 94.9% of the explained variance is maybe attributed to the carbon numbers in each benzene homologue, and 3.7% is related to the chemical structure.[29]

The PCA results of various materials, including benzene homologues, ketone compounds, acids, and others, are shown in Fig. 9.

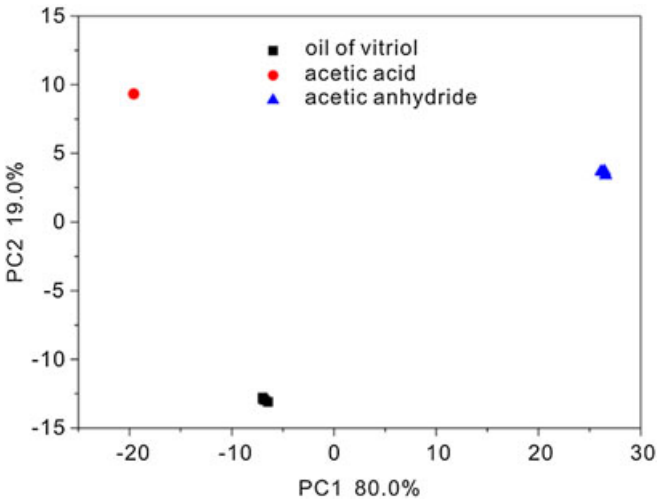

Figure 6. PC1 (80.0%) × PC2 (19.0%) score plot of samples of the different acids.

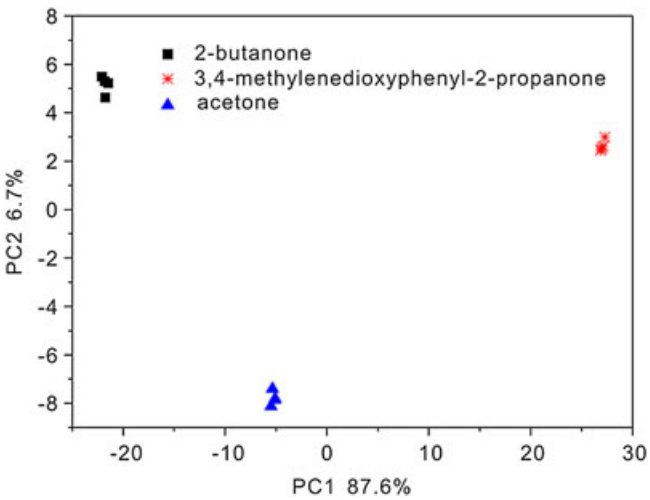

Figure 7. PC1 (87.6%) × PC2 (6.7%) score plot of samples of the different ketone compounds.

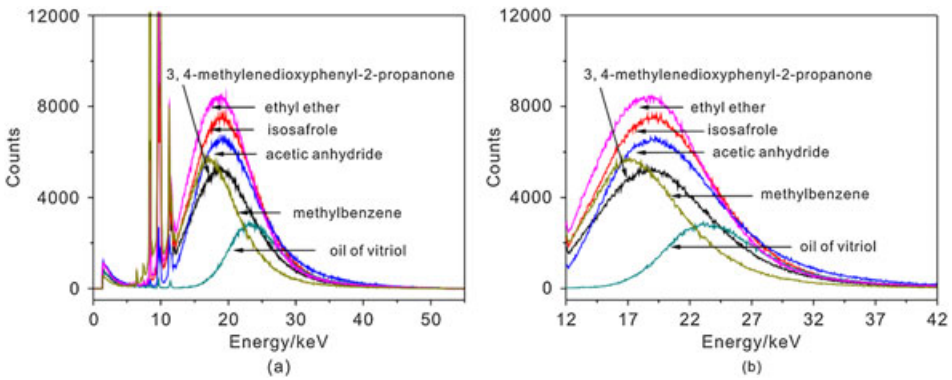

Figure 5. (a) Original X-ray scattering spectra of 3,4-methylenedioxyphenyl-2-propanone, ethyl ether, isosafrole, acetic anhydride, methylbenzene, and oil of vitriol. (b) Expansion of the region of the X-ray scattering used in this work.

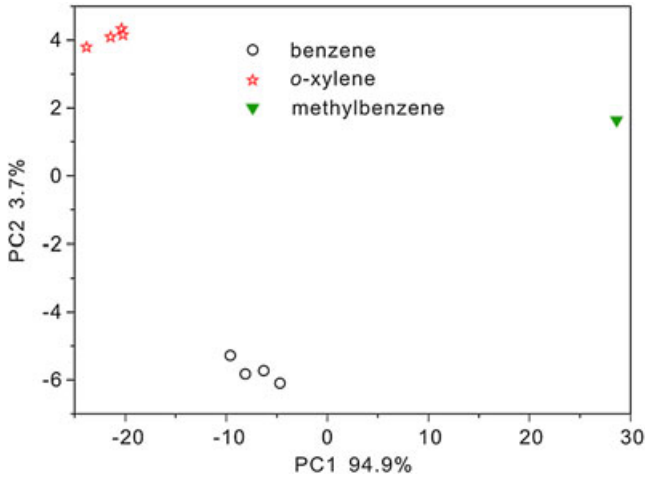

Figure 8. Score plots for PC1 (94.9%) and PC2 (3.7%) showing the good separation among the different benzene homologues.

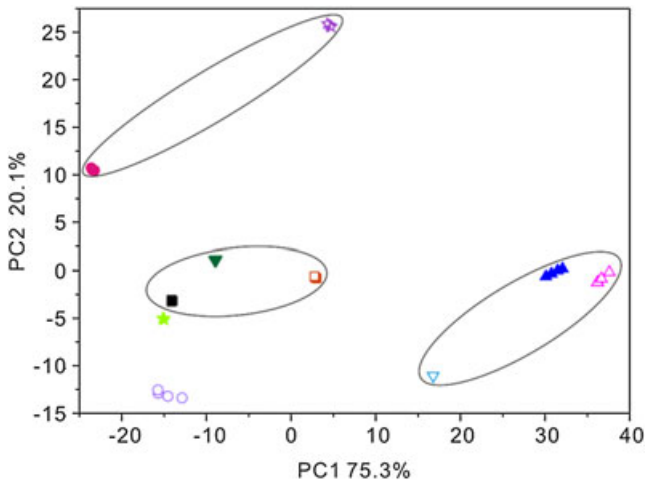

Figure 9. PC1 (75.3%) × PC2 (20.1%) score plots of liquid samples [(▲): benzene; (Δ): *o*-xylene; (▽): methylbenzene; (□): 3,4-methylenedioxyphenyl-2-propanone; (▼): acetone; (■):2-butanone; (⋆): oil of vitriol; (○): ethyl ether; (●): acetic anhydride; (□): isosafrole] after spectral processing by PCA.

It is interesting to note from Fig. 9 that the good separation obtained in the PC1 axis explains 75.3% of the data variance considering the spectral region from 11.93 to 42.13 keV. It is clear from the graph that different materials are separately clustered well. With repeated measurement for four times, the score plots of each substance are clustered together and almost coincident, and it is shown that the spectral data have good repeatability and reliability. At the same time, the different materials can be separated into distinct groups with the different positions. The benzene homologues have large positive values on PC1, the acids have large positive values on PC2, and ketone compounds are located near the origin. The ethyl ether and isosafrole do not mix with benzene homologues, ketone compounds, and acids. On the basis of the aforementioned analysis, it can be concluded that the combination of XRS and PCA offers a valuable method for the classification of liquid precursor chemicals.

Conclusions

The feasibility of using an XRS system combined with PCA for the classification and identification of liquid precursor chemicals has been demonstrated. The XRS spectra of some liquid precursor chemicals and normal materials have been investigated and described in this paper. The analysis of profiles for scattering media distinctly reveals that the XRS spectra are unique to the specific liquid material and significant differences in the liquid substances with similar constituent chemicals can be observed. PCA has been demonstrated as an effective feature extraction method for the XRS spectra of liquid precursor chemicals such as acetone, 2-butanone, 3,4-methylenedioxyphenyl-2-propanone, methylbenzene, acetic anhydride, oil of vitriol, isosafrole, and ethyl ether. This study shows the feasibility of classifying and identifying liquid precursor chemicals by employing XRS and PCA, resulting in a reliable, nondestructive, noncontact experimental and analytical method. These classification and identification are feasible taking into account the similar chemical composition of the liquid precursor chemicals. It can be expected that XRS techniques allied to PCA method will be suitable to identify and classify the suspected liquid fuel and liquid explosives.

Acknowledgements

This work was financially supported by the Key Program of National Natural Science Foundation of China (grant no. 10635070), the Natural Science Foundation of Anhui Provincial Education Department (grant no. KJ2011A269), and the Foundation of Director of the Institute of Intelligent Machines, Chinese Academy of Sciences China.

References

[1] J. S. Lee, W. K. Yang, E. Y. Han, S. Y. Lee, Y. H. Park, M. A. Lim, H. S. Chung, J. H. Park. *Forensic Sci. Int.* **2007**, *173*, 68.
[2] M. Tam, H. H. Hill. *Anal. Chem.* **2004**, *76*, 2741.
[3] Y. Lu, P. B. Harrington. *Anal. Chem.* **2007**, *79*, 6752.
[4] A. C. Oltramari, K. V. Wood, C. Bonham, R. Verpoorte, M. S. B. Caro, A. M. Viana, E. L. Pedrotti, R. P. Maraschin, M. Maraschin. *Plant Cell, Tissue and Organ Culture* **2004**, *4500*, 1.
[5] C. L. O'Neala, D. J. Cprouch, A. A. Fatah. *Forensic Sci. Int.* **2000**, *109*, 189.
[6] G. Harding, J. Delfs. *Proc. SPIE* **2007**, *6707*, 67070T.
[7] G. Harding. *Appl. Radiat. Isot.* **2009**, *67*, 287.
[8] A. Tartari, E. Casnati, C. Baraldi, C. Bonifazzi, G. Maino. *X-ray Spectrom.* **1999**, *28*, 297.
[9] L. Gontrani, F. Ramondo, R. Caminiti. *Chem. Phys. Lett.* **2006**, *417*, 200.
[10] L. Gontrani, F. Ramondo, R. Caminiti. *Chem. Phys. Lett.* **2006**, *422*, 256.
[11] M. Di Marco, M. Port, P. Couvreur, C. Dubernet, P. Ballirano, C. Sadun. *J. Am. Chem. Soc.* **2006**, *128*, 10054.
[12] Y. Zhong, M. Li, B. Sun, J. Wang, F. Zhang, D. Yu, Y. Zhang, J. Liu. *Measurement* **2012**, *45*, 1540.
[13] G. G. Bortoleto, S. S. O. Borges, M. I. M. S. Bueno. *Anal. Chim. Acta* **2007**, *595*, 38.
[14] R. D. Luggar, M. J. Farquharson, J. A. Horrocks, R. J. Lacey. *X-ray Spectrom.* **1998**, *27*, 87.
[15] E. Cook, R. Fong, J. Horrocks, D. Wilkinson, R. Speller. *Appl. Radiat. Isot.* **2007**, *65*, 959.
[16] J. Delfs, J. P. Schlomka. *Appl. Phys. Lett.* **2006**, *88*, 243506.
[17] L. de Oliveira, A. M. Antunes, M. I. M. S. Bueno. *X-ray Spectrom.* **2001**, *39*, 279.
[18] S. Wold, K. Esbensen, P. Geladi. *Chemom. Intell. Lab. Syst.* **1987**, *2*, 37.

[19] F. M. Verbi, E. R. Pereira-Filho, M. I. M. S. Bueno. *Microchim. Acta* **2005**, *150*, 131.
[20] T. L. Alexandre, M. I. M. S. Bueno. *X-ray Spectrom.* **2006**, *35*, 257.
[21] K. Goraieb, T. L. Alexandre, M. I. M. S. Bueno. *X-ray Spectrom.* **2007**, *36*, 241.
[22] L. Luo. *X-ray Spectrom.* **2006**, *35*, 215.
[23] B. Sun, M. Li, F. Zhang, Y. Zhong, N. S. Kang, W. Lu, J. Liu. *Microchem. J.* **2010**, *95*, 293.
[24] C. L. Guo, A. Ji, G. Y. Tao. *Acta Physica Sinica* **1981**, *30*, 1351.
[25] G. Caracciolo, G. Mancini, C. Bombelli, P. Luciani, R. Caminiti. *J. Phys. Chem. B* **2003**, *107*, 12268.
[26] R. D. Luggar, M. J. Key, E. J. Morton, W. B. Gilboy. *Nucl. Instr. Meth. Phys. Res. A* **1999**, *422*, 938.
[27] K. Ellmer, R. Mientus, V. Weiss, H. Rossner. *Meas. Sci. Technol.* **2003**, *14*, 336.
[28] R. D. Luggar, J. A. Horrocks, R. D. Speller, R. J. Lacey. *Appl. Radiat. Isot.* **1997**, *48*, 215.
[29] M. I. M. S. Bueno, M. T. P. O. Castro, A. M. de Souza, E. B. S. de Oliveira, A. P. Teixeira. *Chemometrics Intell. Lab. Syst.* **2005**, *78*, 96.

